Supporting Information

$LaMn_3Ni_2Mn_2O_{12}$: An A- and B-site Ordered Quadruple Perovskite with A-site Tuning Orthogonal Spin Ordering

Yun-Yu Yin,[†] Min Liu,[†] Jian-Hong Dai,[†] Xiao Wang,[†] Long Zhou,[†] Huibo Cao,[‡] Clarina dela Cruz,[‡] Chien-Te Chen,[§] Yuanji Xu,[†] Xi Shen,[†] Richeng Yu,[†] José Antonio Alonso,[∥] Angel Muñoz,[⊥] Yi-feng Yang,*[,†,#] Changqing Jin,[†,#] Zhiwei Hu,[▽] and Youwen Long*[,†,#]

[†]Beijing National Laboratory for Condensed Matter Physics, Institute of Physics, Chinese Academy of Sciences, Beijing 100190, China

[‡]Quantum Condensed Matter Division, Neutron Scattering Science Directorate, Oak Ridge National Laboratory, Oak Ridge, Tennessee 37831, USA

[§]National Synchrotron Radiation Research Center, Hsinchu 30076, Taiwan, R.O.C

[∥]Instituto de Ciencia de Materiales de Madrid, C.S.I.C., Cantoblanco, Madrid E-28049, Spain

[⊥]Universidad Carlos III, Avenida Universidad 30, E-28911, Leganés-Madrid, Spain

[#]Collaborative Innovation Center of Quantum Matter, Beijing 100190, China

[▽]Max Planck Institute for Chemical Physics of Solids, Dresden 01187, Germany

Magnetic structure resolution by neutron powder diffraction

Group theory analysis

The magnetic structure of LMNM has been analyzed from the NPD patterns acquired at T = 40 K and T = 3 K. In the NPD pattern obtained at T = 40 K new reflections are observed at Bragg positions which are not allowed by the *Pn*-3 space group, such as the (100) and (210) Bragg reflections. It indicates that the propagation vector characterizing the magnetic structure is k = 0 and the chemical and the magnetic unit cells coincide. The same magnetic reflections are observed in the NPD pattern acquired at T = 3 K, except that their intensity has increased, indicating that the propagation vector is also k = 0 at 3 K.

In the resolution of the magnetic structure, the different solutions which are compatible with the symmetry of the nuclear structure of LMNM have been considered. These solutions have been determined by following the representation analysis technique described by Bertaut.[S1] The different solutions have been calculated by using the program SARAh.[S2] For k = 0, the small group G_k coincides with the cubic *Pn*-3 space group. G_k has eight irreducible representations. There are three magnetic sites in LMNM, which are susceptible to present a magnetic ordering. For the 6*d* site, occupied by Mn^{3+} ions, the six atoms of the site are denoted by Mn1 (1/4, 3/4, 3/4); Mn2 (3/4, 3/4, 1/4); Mn3 (3/4, 1/4, 3/4); Mn4 (3/4, 1/4, 1/4); Mn5 (1/4, 1/4, 3/4) and Mn6 (1/4, 3/4, 1/4). For the 4*b* site, occupied by Ni^{2+} ions, the notation is Ni1 (0, 0, 0); Ni2 (0, 1/2, 1/2); Ni3 (1/2, 0, 1/2) and Ni4 (1/2, 1/2, 0). Finally, for the 4*c* site, occupied by the Mn^{4+}, the four atoms are denoted by Mn7 (1/2, 1/2, 1/2); Mn8 (1/2, 0, 0); Mn9 (0, 1/2, 0) and Mn10 (0, 0, 1/2). A Γ representation is constructed for each of the sites with the magnetic moments of the atoms that occupy the different positions associated with each site. These representations are decomposed in terms of the eight irreducible representations of the small group G_k, in this case *Pn*-3. For the sites 6*d*, 4*b* and 4*c* the decompositions are:

$\Gamma_{6d} = 3\Gamma^7 + 3\Gamma^8$;

$\Gamma_{4b} = \Gamma^1 + \Gamma^3 + \Gamma^5 + 3\Gamma^7$;

$\Gamma_{4c} = \Gamma^1 + \Gamma^3 + \Gamma^5 + 3\Gamma^7$;

The irreducible representations Γ^1, Γ^3 and Γ^5 are one-dimensional, whereas Γ^7 and Γ^8 are of order three. The basis vectors associated with the different irreducible representations and sites are presented in Table S1 and S2. According to Table S1, for the Mn^{3+} ions occupying the 6*d* site, the group theory only establishes a relationship between those atoms related by the inversion symmetry element. For Γ^7 the coupling between the magnetic moments of each pair is ferromagnetic (FM) and for Γ^8 the coupling is antiferromagnetic (AFM). However, it is expected that all the atoms belonging to the same 6*d* site will have the same magnetic moment. It would imply new relationships between the basis vectors, such as $\Psi_{17} = \pm\Psi_{47} = \pm\Psi_{77}$; $\Psi_{27} = \pm\Psi_{57} = \pm\Psi_{87}$; $\Psi_{37} = \pm\Psi_{67} = \pm\Psi_{97}$. Similar relationships can be established among the basis vectors of Γ^8. As regarding the possible solutions for the 4*b* and 4*c* sites (Ni^{2+} and Mn^{4+}, respectively), according to Table S2, the basis vectors are similar for both sites, so the relationships among the magnetic moments of the atoms belonging to the same site are the same. For Γ^1, Γ^3 and Γ^5 the coupling is AFM. For Γ^7 the coupling is more complex, as it is given by the combinations of 9 basis vectors.

Table S1. Basis vectors (BVs) for the 6*d* site occupied by the Mn^{3+} ions.

	BV	Mn1	Mn4	BV	Mn2	Mn5	BV	Mn3	Mn6
Γ^7	Ψ_{17}	(100)	(100)	Ψ_{47}	(100)	(100)	Ψ_{77}	(100)	(100)
	Ψ_{27}	(010)	(010)	Ψ_{57}	(010)	(010)	Ψ_{87}	(010)	(010)
	Ψ_{37}	(001)	(001)	Ψ_{67}	(001)	(001)	Ψ_{97}	(001)	(001)
Γ^8	Ψ_{18}	(100)	(-100)	Ψ_{48}	(100)	(-100)	Ψ_{78}	(100)	(-100)
	Ψ_{28}	(010)	(0-10)	Ψ_{58}	(010)	(0-10)	Ψ_{88}	(010)	(0-10)
	Ψ_{38}	(001)	(00-1)	Ψ_{68}	(001)	(00-1)	Ψ_{98}	(001)	(00-1)

Table S2. Basis vectors (BVs) for the 4*b* and 4*c* sites occupied by the Ni^{2+} and Mn^{4+} ions, respectively. The possible solutions are the same for both sites.

	BV	Ni1 Mn7	Ni2 Mn8	Ni3 Mn9	Ni4 Mn10
Γ^1	Ψ_{11}	(111)	(1-1-1)	(-11-1)	(-1-11)
Γ^3	Ψ_{13}	(1-10)	(110)	(-1-10)	(-110)
Γ^5	Ψ_{15}	(11-2)	(1-12)	(-112)	(-1-1-2)
Γ^7	Ψ_{17}	(111)	(1-1-1)	(1-11)	(11-1)
	Ψ_{27}	(1-10)	(110)	(110)	(1-10)
	Ψ_{37}	(11-2)	(1-12)	(1-1-2)	(112)
	Ψ_{47}	(111)	(-111)	(-11-1)	(11-1)
	Ψ_{57}	(01-1)	(01-2)	(011)	(011)
	Ψ_{67}	(-211)	(211)	(21-1)	(-211)
	Ψ_{77}	(111)	(-111)	(1-11)	(-1-11)
	Ψ_{87}	(-101)	(101)	(-101)	(101)
	Ψ_{97}	(1-21)	(-1-21)	(121)	(-121)

Magnetic structure refinement results

Table S3. Results from the fitting of the magnetic structure (2θ range: 8.5-70º).

		Mn (6*d*)	Ni (4*b*)	Mn (4*c*)
	Solution	$m_{1x}=m_{2x}=m_{3x}=-m_{4x}$ $=-m_{5x}=-m_{6x}$; $m_{iy}=m_{iz}=0$		
T = 40 K	Values	m_{1x} = 1.60(8) μ_B |m| = 1.60(8) μ_B	-------	--------
	Fitting Parameters		R_B = 3.97 R_{Mag} = 13.7 χ^2 = 2.39	
	Solution	$m_{1x}=m_{2x}=m_{3x}=-m_{4x}$ $=-m_{5x}=-m_{6x}$; $m_{iy}=m_{iz}=0$	$m_{7x}=m_{8x}=m_{9x}=m_{10x}=u$; $m_{7y}=-m_{8y}=-m_{9y}=m_{10y}=-u$; $m_{iz}=0$	$m_{11x}=m_{12x}=m_{13x}=m_{14x}=v$; $m_{11y}=-m_{12y}=-m_{13y}=m_{14y}=-v$; $m_{iz}=0$
T = 3 K	Values	m_{1x} = 2.94(8) μ_B |m| = 2.94(8) μ_B	u = 0.46(3) μ_B |m| = 0.65(3) μ_B	v = 0.31(12) μ_B |m| = 0.44(3) μ_B
	Fitting Parameters		R_B = 8.88 R_{Mag} = 8.95 χ^2 = 6.26	

Density functional theory calculations

Electronic structure

We calculated the electronic structure of LMNM with GGA+*U* method (without considering spin-orbit coupling effects) based on the non-collinear magnetic structure determined by the low-temperature NPD. The calculated density of states (DOS) and band structure are shown in Figure 8b. The 3*d* states of A′-site Mn, B-site Ni and B′-site Mn cations show very large overlap, indicating that the intersite exchange interactions between A′- and B/B′-sites are comparable to the A′−A′ and B/B′−B/B′ exchange interactions. The calculated magnetic moments of A′-site Mn^{3+}, B-site Ni^{2+} and B′-site Mn^{4+} are 3.56, 1.70 and 2.83 μ_B, respectively, which are reasonably consistent with the values expected from their valences. The remaining moments are 0.08 μ_B at the O site. As show in the DOS, the Fermi level lies in the energy gap, indicting the insulating behavior of LMNM, which is in well agreement with the experiment.

Exchange interactions

In order to get a deep insight into the complex magnetic exchange interactions in LMNM, we calculated the strength of exchange interactions J_1-J_8 between Mn^{3+}, Ni^{2+} and Mn^{4+} spins, with the exchange path ways shown in Figure 8a. We have performed spin-polarized DFT+*U* calculations with 9 different collinear magnetic configurations: (1) FM, (2) FiM1, (3) FiM2-A, (4) FiM2-B, (5) FiM3, (6) FiM4-A, (7) FiM4-G, (8) FiM5, (9) FiM6, which are schematically shown in Figure S2. All these calculations were done on one single unit cell. We have mapped the total energy of the above magnetic configurations into the Heisenberg model. The equation was given by eqaution

$$H = E_0 - \sum_{i<j} J_{ij} \vec{S}_i \cdot \vec{S}_j \quad \text{(S1)},$$

where E_0 is a sum of the nonmagnetic part. J_{ij} are the exchange constants for exchange interaction between spin S_i and S_j at sites i and j, respectively.[S3] The positive (negative) J_{ij} represents FM (AFM) coupling of the two spins. We found that the system energy of both the nonlinear spin structure determined in experiment and the linear FM one is comparable and most stable compared to others.

For simplicity, we have expressed J_{ij} in terms of J_1−J_8 for different pairs of Mn−Mn, Ni−Ni and Mn−Ni interactions. Here, we used $S_1 = 2$, $S_2 = 1$ and $S_3 = 3/2$ for the A′-site Mn^{3+}, B-site Ni^{2+} and B′-site Mn^{4+}, respectively.

The Hamiltonian above have 9 unknown parameters: E_0 and J_1−J_8. The equations corresponding to the above 9 magnetic configurations were listed as the set of Eqs. S2-S10 by one formula. A least-squares fitting method was also used to determine these values,

$$E(FM) = E_0 - 6J_1S^2_1 - 12J_2S^2_1 - 12J_3S^2_1 - 12J_4S_2\cdot S_3 - 12J_5S^2_2 - 12J_6S^2_3 - 12J_7S_1\cdot S_2 - 12J_8S_1\cdot S_3 \quad (S2)$$

$$E(FiM1) = E_0 - 6J_1S^2_1 - 12J_2S^2_1 - 12J_3S^2_1 + 12J_4S_2\cdot S_3 - 12J_5S^2_2 - 12J_6S^2_3 - 12J_7S_1\cdot S_2 + 12J_8S_1\cdot S_3 \quad (S3)$$

$$E(FiM2\text{-}A) = E_0 - 2J_1S^2_1 + 4J_2S^2_1 + 12J_3S^2_1 + 12J_4S_2\cdot S_3 - 12J_5S^2_2 - 12J_6S^2_3 \quad (S4)$$

$$E(FiM2\text{-}B) = E_0 + 2J_1S^2_1 + 4J_2S^2_1 - 4J_3S^2_1 + 12J_4S_2\cdot S_3 - 12J_5S^2_2 - 12J_6S^2_3 \quad (S5)$$

$$E(FiM3) = E_0 - 6J_1S^2_1 - 12J_2S^2_1 - 12J_3S^2_1 - 4J_4S_2\cdot S_3 + 4J_5S^2_2 + 4J_6S^2_3 \quad (S6)$$

$$E(FiM4\text{-}A) = E_0 - 2J_1S^2_1 + 4J_2S^2_1 + 12J_3S^2_1 - 12J_4S_2\cdot S_3 - 12J_5S^2_2 - 12J_6S^2_3 \quad (S7)$$

$$E(FiM4\text{-}G) = E_0 + 6J_1S^2_1 - 12J_2{}^2S^2_1 + 12J_3S^2_1 - 12J_4S_2\cdot S_3 - 12J_5S^2_2 - 12J_6S^2_3 \quad (S8)$$

$$E(FiM5) = E_0 - 6J_1S^2_1 - 12J_2S^2_1 - 12J_3S^2_1 - 12J_4S_2\cdot S_3 - 12J_5S^2_2 - 12J_6S^2_3 + 12J_7S_1\cdot S_2 + 12J_8S_1\cdot S_3 \quad (S9)$$

$$E(FiM6) = E_0 - 6J_1S^2_1 - 12J_2S^2_1 - 12J_3S^2_1 + 4J_4S^2_2 - 12J_6S^2_3 - 12J_8S_1\cdot S_3 \quad (S10)$$

We use the effective spin exchange constants $J_{ij}^{eff} = J_{ij}\, S_i\cdot S_j$ to compare the relative strengths of the spin exchange interactions between Mn^{3+}, Ni^{2+} and Mn^{4+}ions. The calculated values are listed in Figure 8a. According to these values, it is obvious that the effective exchange constants J_1^{eff}, J_2^{eff} and J_3^{eff}, respectively, corresponding to the NN, NNN and TNN exchange interactions between A′(Mn^{3+})−A′(Mn^{3+}) spins, are all AFM. While the exchange interactions B(Ni^{2+})−B′(Mn^{4+}) J_4^{eff}, B(Ni^{2+})−B(Ni^{2+}) J_5^{eff} and B′(Mn^{4+})−B′(Mn^{4+}) J_6^{eff} are all FM. These calculated results all are consistent with the experiments.

The intersite exchange interactions A′(Mn^{3+})−B(Ni^{2+}) J_7^{eff} is FM while A′(Mn^{3+})−B′(Mn^{4+}) J_8^{eff} is AFM, indicating there being a competition between these two interactions. These comparable FM and AFM exchange interactions occurring in the A′-site Mn^{3+}, B-site $Ni^{2+}$and B′-site Mn^{4+} spins can

form a geometrical magnetic triangle. We mainly attribute the highly non-collinear magnetic structure at the B/B′-sublattices to be the result of the competition in these magnetic triangles.

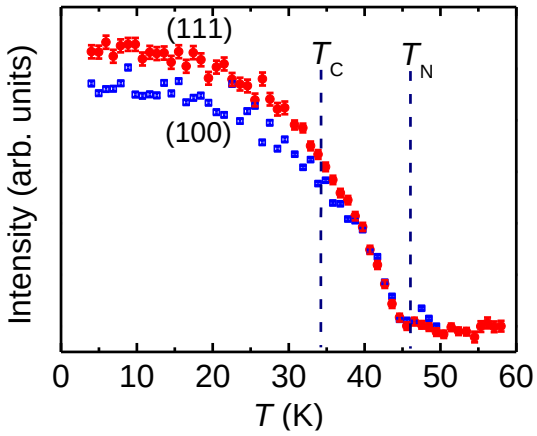

Figure S1. Normalized neutron diffraction intensity as a function of temperature for (100) and (111) peaks. These two curves sharply increase at T_N and then tend to separate for each other below T_C.

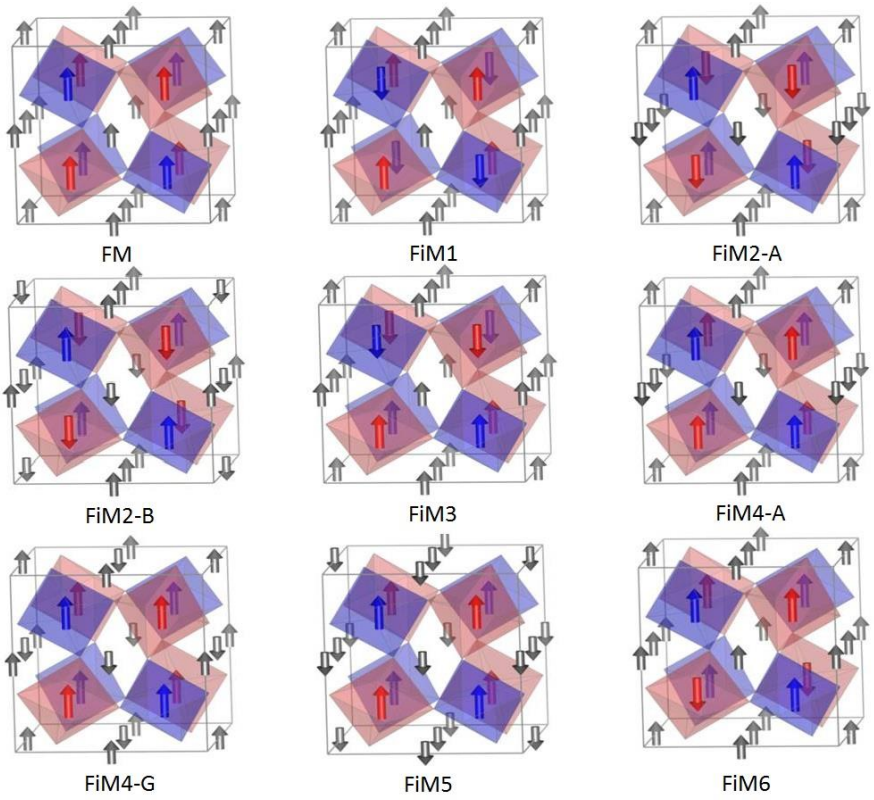

Figure S2. Schematic view of the 9 collinear spin arrangements of the A′-site Mn^{3+} (gray), B-site Ni^{2+} (red), and B′-site Mn^{4+} (blue) and in LMNM

REFERENCE

[S1] Bertaut, E. F.; *Magnetism*, Rado, G. T.; Shul, H. Eds Academic: New York, Vol. III, Chapter 4, 1963.

[S2] Willis, A. S. A New Protocol for the Determination of Magnetic Structures using Simulated Annealing and Representational Analysis (SARA*h*). *Physica B* **2000**, *276*, 680–681.

[S3] Anderson, P. W. *Theory of Magnetic Exchange Interactions*: *Exchange in Insulators and Semiconductors*, edited by Seitz, F. and Turnbull, D. *Solid State Physics* Vol. 14 (Academic, New York, 1963), pp. 99-214.